DISINTEGRATION OF THE NUCLEAR SYSTEM FORMED IN THE 45 MeV/NUCLEON ^{84}Kr + ^{159}Tb REACTION

Z. Majka[1], L. G. Sobotka, D.W. Stracener, D.G. Sarantites

Department of Chemistry, Washington University
St. Louis, Missouri 63130

G. Auger, E. Plagnol, Y. Schutz

GANIL, BP 5027, F14021 Caen Cedex, France

R. Dayras, J.P. Wieleczko

CEN-Saclay, F91191, Gif-sur-Yvette Cedex, France

J. Barreto

Institut de Physique, Nucleare-BP01-91406-Orsay Cedex, France

E. Norbeck

Department of Physics, University of Iowa
Iowa City, Iowa 52242

ABSTRACT

The occurrence of exit channels for which no massive remnant of either the target or projectile is established for 45 MeV/Nucleon ^{84}Kr reaction on ^{159}Tb. Up to 11 intermediate mass fragments were detected in coincidence with high multiplicity of light charge particles. Several characteristics of multifragment exit channels are investigated.

One of the most stimulating and challenging aspects of the intermediate - energy heavy ion collision studies is the observed growth of intermediate mass fragment (IMF) production with beam energy. A variety of models has been proposed for complex fragment formation mechanisms ranging from the binary

[1] Permanent Address: Institute of Physics, Jagellonian University, PL30053, Krakow, Poland

decay mechanism[1] to a large group of multifragmentation mechanisms.[2] On the other hand, very little experimental data are available (those that are mostly single fragment inclusive measurements) and an unambiguous verification of the models has not been feasible up to the present time. An event-by-event coincidence measurement of all reaction products with a large solid angle acceptance is required in order to understand fragment formation mechanism. Only recently, the LBL/GSI Plastic-Ball-Wall detector system was used to study light charge particles (LCP) and IMF emission over a large solid angle in 200 MeV/nucleon heavy ion collisions at Bevalac.[3] However, at energies between 55 and 110 MeV/nucleon, a direct observation of events with the complete explosion of the system was reported in emulsion experiments for the ^{12}C induced reaction in Ag(Br).[4]

In this contribution we report for the first time observation of the complete disintegration of colliding nuclei at 45 MeV/Nucleon ^{84}Kr induced reaction on ^{159}Tb. Using a 4π type detection system we selected a subset of events for which the total undetected charge in each event is smaller than one third of the target nucleus charge. The characteristics of these events suggest that they originate from a different process than those observed together with a heavy remnant.

The experiment was performed at the GANIL facility. A 45 MeV/nucleon ^{84}Kr beam was used to bombard several targets (^{12}C, ^{27}Al, ^{45}Sc, ^{84}Nb, ^{159}Tb and ^{181}Ta) placed in the Cyrano scattering chamber. In this

contribution we report the results for the ^{84}Kr + ^{159}Tb reaction. The IMF's and LCP's were detected with the 103 element phoswich detector system, of the "Dwarf-Ball-Wall", developed at Washington University.[5] Each phoswich detector consisted of a thin fast plastic scintillator foil followed by a thick CsI(Tl) scintillator. The thickness of the fast plastic scintillators varies from 200 μm to 10 μm for the detectors between 8° and 156°. The thicknesses of the CsI(Tl) detectors also vary with angle, being 20 mm for angles between 8° and 25°, 8 mm between 35° and 56° and 4 mm for angles greater than 56°. In order to suppress secondary electrons and X-rays the detectors located at $\theta >$ 60° and the detectors located at 12° $< \theta <$ 60° were covered by Au foils of 1.7 mg/cm^2 thick and Ta foils of 7.4 mg/cm^2, respectively. The most forward detectors at $\theta <$ 12°, were shielded by Ta of 10 g/cm^2. These absorbers lowered the efficiency for the detection of the IMF's, but still allowed for the detection of LCP's. Two opposite detectors have been replaced by two small entrance and exit beam tubes which act as cleanup collimators. Two additional elements were removed for insertion of the target and viewing a scintillator in the target position, which was used for beam focusing. The detection array provided an angular coverage corresponding to approximately 93% of 4π.

The system was employed in a self-triggering mode. Isotopic identification for the LCP's ($Z \leq 2$) and elemental identification of the IMF's up to $Z = 24$ was obtained by integrating the photomultiplier anode current during three different time intervals. This information was also used to obtain

the energy of the LCP's. The detection thresholds vary from 3.8 MeV to 1.0 MeV for protons and from 15.0 MeV to 3.6 MeV and for alpha particles from the most forward to the most backward angles. All heavier fragments which passed through the absorber were included in the multiplicity determination even when they stopped in the plastic scintillator foils. The resulting detection thresholds varied from 1.8 MeV/nucleon to 0.4 MeV/nucleon for the forward and the backward angles, respectively.

In Figure 1 we have plotted the distribution of total charge (thick solid

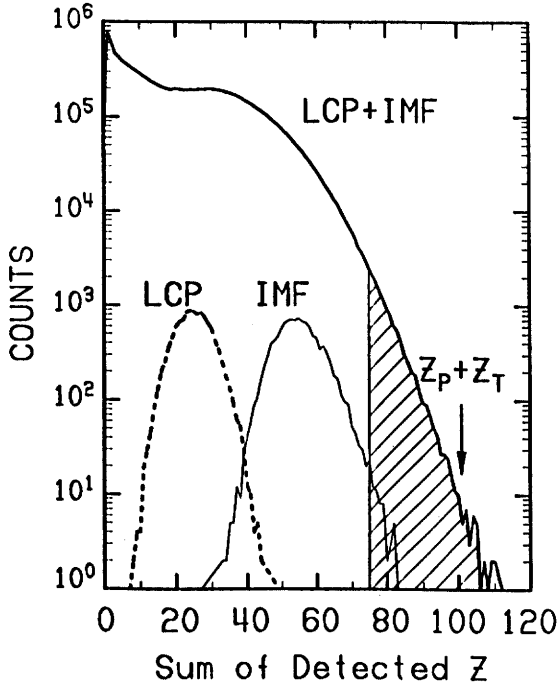

Figure 1. Total detected charge distribution (thick solid line). Distributions of detected charge in the LCP's and the IMF's for the shaded area of the total detected charge are given by dashed and thin solid lines, respectively.

line) detected by Dwarf-Ball-Wall system. One can see that in this measurement a significant number of events were recorded for which more than 75% of total charge of the projectile and target nuclei ($Z_{Tot} = Z_p + Z_T = 101$) was detected (shaded area in Figure 1). Distributions of the detected charge in the LCP's (dashed line) and in the IMF's (thin solid line) for this subset of events are also shown in Figure 1. Here we observe that as much as one-third of the total detected charge is in the form of the LCP's.

The LCP multiplicity, M_{LCP}, as a function of the multiplicity of the IMF's, M_{IMF}, is shown in Figure 2*a*.

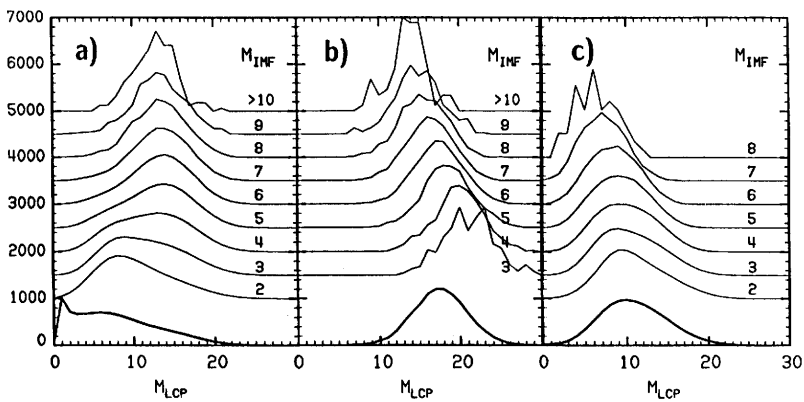

Figure 2. *a)* The LCP multiplicities (thick solid lines) and correlation between the multiplicity of the IMF and the LCP multiplicities (thin solid lines). *b)* The same as *(a)* but for $Z_{det} > 75$. *c)* The same as *(a)* but for $20 < Z_{det} < 45$.

One can see that the M_{LCP} distributions have two components (see Figure 2*a*). When only a few IMF's are detected the M_{LCP} distributions peak at rather low

value ($M_{LCP} < 8$). As the number of detected IMF's is increased the M_{LCP} distributions become broader, almost flat-topped, and extend to considerably higher values. For still larger M_{IMF} values, the M_{LCP} distributions regain a peaked form but with substantially greater mean value than for the distribution for the low M_{IMF} values. In Figure 2(*b*) and (*c*) we again plot the correlation between the IMF multiplicity and the LCP multiplicity, however, with the requirement that the total detected charge is greater than 75% of Z_{Tot} (Figure 2*b*) or that $20 < Z_{det} < 45$ (Figure 2*c*). Here we observe one component distributions of the M_{LCP} which peak at high/low values for a large/small value of the total detected charge, respectively.

Since the detection system is efficient for the detection of light ions but becomes more inefficient as the charge increases and the ion velocity decreases (due to absorbers), the events with low values of total detected charge must be associated with one or a few undetected massive heavy ions. This suggests that the component of the M_{LCP} distribution in coincidence with only a few IMF's, which also tends to have a large deficit in the total detected charge, results from deep inelastic like or fusion events in which a massive residue survives but escapes detection. On the other hand, the component of the M_{LCP} distribution in coincidence with several IMF's is associated with well characterized ($Z_{det} > 75$) nuclear explosions with no surviving very massive remnant.

In the second part of this contribution we will investigate selected properties of this subset of events for which large amounts of the total charge

was detected (Z_{det} > 75). This subset of events selects the collisions where there is almost complete disintegration of the nuclear system into a large number of small pieces. Figure 3*a* shows the multiplicity distributions for the

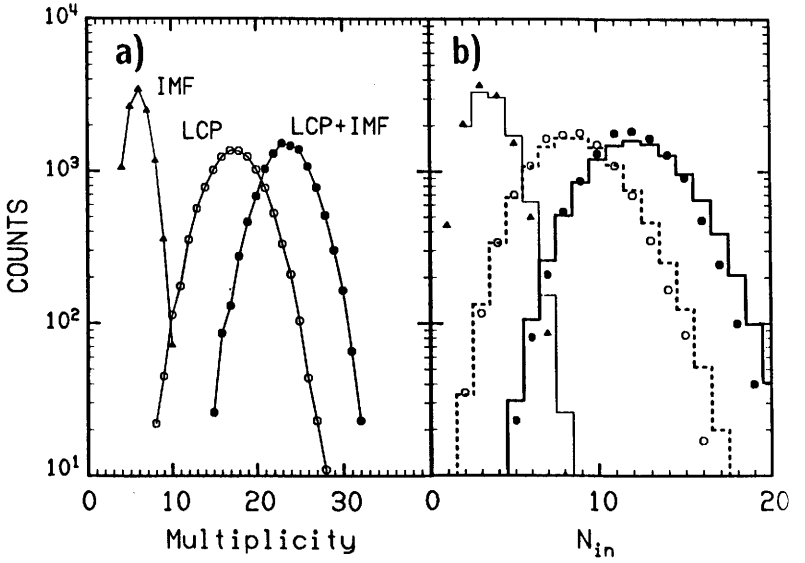

Figure 3. The multiplicity distributions of LCP's, IMF's and total, when the total detected charge is ≥ 75, are shown in part a). The symbols in part b) correspond to the number of ions , N_{in} which are within ±45° of the plane defined by the beam and the ion with the largest charge. The histograms are the result of folding of the multiplicity distributions of part a) with binomial distributions with a chance probability of p = ½.

IMF's (triangles), the LCP's (open symbols) and the total (dots) for the subset of events described above. Three characteristic features of these distributions are: *(1)* The IMF's multiplicity distribution is narrow, peaks at M_{IMF} = 6 and extends up to 11 IMF's per event. *(2)* The LCP's multiplicity distribution is

broad ($6 < M_{LCP} < 28$) and peaks at 18 per event. *(3)* The high multiplicity of the IMF's is correlated with the large LCP's multiplicity (see Figure 2*b*).

The spatial distribution of event fragments was investigated by determining the number of ions $N_{i,in}$ (i = IMF's, LCP's and total) which were within 45° of the plane determined by the beam axis and the direction of the heaviest IMF of each event. These are shown as symbols in Figure 3*b*. The mean values are close to 1/2 of those observed in Figure 3*a* suggesting a random spatial distribution of ions in each event. This was verified by folding the experimental multiplicity distributions in Figure 3*a* with a binomial distribution with a chance probability p = 1/2. The agreement between the folded distributions (histograms in Figure 3*b*) and the experimental data (symbols in Figure 3*b*) is almost perfect indicating that for these events the fragments are randomly distributed with respect to the azimuthal angle.

The elemental distribution of the IMF's, presented in Figure 4, was fitted with a power law,[6] $P(Z_{IMF}) \sim Z_{IMF}^{\tau}$, where, τ, is the apparent exponent. This fit is extended over the region $5 \leq Z_{IMF} \leq 15$. The yield of Z = 4 was excluded because it is depressed due to the fact that ^{8}Be is particle unstable. The upper limit, Z = 15 results from the considerable loss of efficiency for heavy low velocity ions. The results of the fits and the apparent exponents are given in Figure 4. This value is less than those extracted from inclusive studies.[7] The distribution of the heaviest fragments for this subset of events is also presented in Figure 4 (filled symbols). For reference, the temperature of the

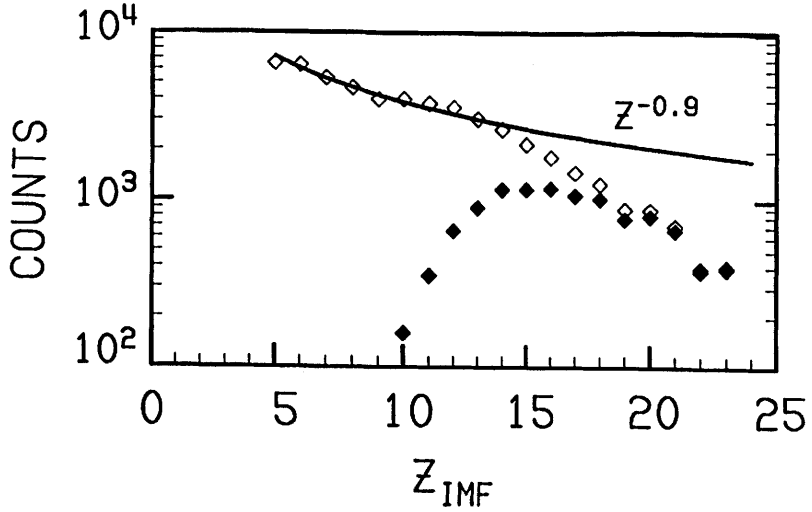

Figure 4. The elemental distribution of IMF's (open diamonds) for events with $Z_{det} > 75$. The distribution of the heaviest fragments in this subset of events are shown by filled symbols. Solid line represents a power low fit.

system should be between 11.2 MeV (full momentum transfer) and 9.5 MeV (46 beam velocity particles emitted).[8] For each case a level density parameter was taken for hot nuclear matter.[9]

In summary, we established the occurrence of multifragment disintegration of the nuclear system formed in the 45 MeV/nucleon ^{84}Kr + ^{158}Tb reaction. For this subset of events no heavy remnant survives the collision. High LCP multiplicity, a low value of the apparent exponent and a uniform emission distribution in the plane perpendicular to the beam are the characteristics which differentiate these events from those with heavy remnant in the exit channel. Further studies which are in progress address the question of whether these observations indicate the occurrence of a liquid gas phase transition.

REFERENCES

1. R. Charity *et al.*, *Nucl. Phys.*, 225c (1987).

2. J. Hufner, *Phys. Rep.*, 125, 129 (1985); L. Csernai and J. Kapusta, *Phys. Rep.*, 131, No. 6 (1986).

3. B.V. Jacak *et al.*, *Nucl. Phys.*, A488, 325c (1988).

4. N. Jakobson *et al.*, *Z. Phys.*, A307, 293 (1982).

5. D.G. Sarantites *et al.*, *Nucl. Inst. and Meth.*, A264, 319 (1988).

6. M.E. Fisher, *Physics (G.B.)* 3, 255 (1967).

7. A.D. Panagioton *et al.*, *Phys. Rev.* C31, 55 (1985).

8. C. Cerruti *et al.*, *Nucl. Phys.* A476, 74 (1988).

9. G. Nebbia *et al.*, *Phys. Lett.* 176B, 20 (1986).